Title

Cerebral and Muscle Tissue Oxygenation During Incremental Cycling in Male Adolescents Measured by Time-Resolved Near-Infrared Spectroscopy.

Journal

Pediatric Exercise Science, 28(2)

ISSN

0899-8493

Authors

Ganesan, Goutham
Leu, Szu-yun
Cerussi, Albert
et al.

Publication Date

2016-05-01

DOI

10.1123/pes.2015-0037

Peer reviewed

HHS Public Access

Author manuscript

Pediatr Exerc Sci. Author manuscript; available in PMC 2017 May 01.

Published in final edited form as:

Pediatr Exerc Sci. 2016 May ; 28(2): 275–285. doi:10.1123/pes.2015-0037.

Cerebral and Muscle Tissue Oxygenation During Incremental Cycling in Male Adolescents Measured by Time-Resolved NIRS

Goutham Ganesan[1], **Szu-yun Leu**[1], **Albert Cerussi**[2], **Bruce Tromberg**[2], **Dan M. Cooper**[3], and **Pietro Galassetti**[3]

[1]Institute for Creative Technologies; University of California, Irvine, CA

[2]Beckman Laser Institute; University of California, Irvine, CA

[3]Department of Pediatrics & Institute for Clinical and Translational Science; University of California, Irvine, CA

Abstract

Near-infrared spectroscopy (NIRS) has long been used to measure tissue-specific O_2 dynamics in exercise, but most published data have used continuous wave devices incapable of quantifying absolute Hemoglobin (Hb) concentrations. We used time-resolved NIRS (TR-NIRS) to study exercising muscle (Vastus Lateralis, VL) and prefrontal cortex (PFC) Hb oxygenation in 11 young males (15.3 ± 2.1 yrs) performing incremental cycling until exhaustion (peak VO2 = 42.7 ± 6.1 ml/min/kg, mean peak power = 181 ± 38 W). TR-NIRS measurements of reduced scattering (μ_s') and absorption (μ_a) at three wavelengths (759, 796, and 833 nm) were used to calculate concentrations of oxyHb ([HbO_2]), deoxy Hb ([HbR]), total Hb ([THb]), and O_2 saturation (stO_2). In PFC, significant increases were observed in both [HbO_2] and [HbR] during intense exercise. PFC stO_2% remained stable until 80% of total exercise time, then dropped (−2.95%, p = .0064). In VL, stO_2% decreased until peak time (−6.8%, p = .01). Segmented linear regression identified thresholds for PFC [HbO_2], [HbR], VL [THb]. There was a strong correlation between timing of second ventilatory threshold and decline in PFC [HbO_2] (r = .84). These findings show that TR-NIRS can be used to study physiological threshold phenomena in children during maximal exercise, providing insight into tissue specific hemodynamics and metabolism.

Keywords

NIRS; Exercise; Oxygenation

Introduction

The recent emphasis on the importance of exercise in health promotion and disease prevention has been paralleled by the necessity for novel, more comprehensive exercise testing tools. Incremental cardio-pulmonary exercise testing (CPET) is the established gold-standard to assess fitness in adults and children (45). There is increasing awareness, however, of its limitations in detecting subtle physiological factors affecting performance, such as oxygenation changes in relevant cerebral areas (29), altered muscle microvascular perfusion (8), and the relative contributions of skeletal muscles and central nervous system in determining maximal performance (2). In general terms, therefore, exercise testing

methodologies allowing the study of tissue-specific physiology during exertion may provide novel, necessary mechanistic insights into the beneficial effects of exercise. In this context, Near-infrared spectroscopy (NIRS), a technique capable of assessing hemoglobin (Hb) content and oxygenation *in vivo* is proving to be an increasingly powerful tool (11, 23). Among the basic physiological applications for NIRS measurements in skeletal muscles are the study of the mechanisms underpinning muscle oxygen uptake kinetics in relation to pulmonary function (25, 26, 38), modeling changes in skeletal muscle blood flow (15, 18), and assessment of muscle fatigue (40). Additionally, neurological responses to exercise can also be non-invasively studied with NIRS, with the goal of understanding cerebral vascular regulation (2), or elucidating central mechanisms governing exercise performance (12). There is still relatively little known about these central mechanisms in children, and their potential role in regulating motivation and perceived exertion (41).

While NIRS is particularly useful in children because it is noninvasive and safe, there are many outstanding issues that must be addressed with regard to different NIRS approaches, as well as data interpretation. For example, the impact of changes in tissue scattering and optical path length in the context of exercise has not been fully investigated. Published NIRS studies typically employ continuous wave devices, whose main limitation is the inability to account for such changes, which is required for absolute quantitation of hemoglobin content and oxygenation. Most of these published studies have been able to describe temporal patterns in NIRS data during exercise (34), but the lack of absolute quantitation has rendered it difficult to assess the magnitude of such changes, and to compare values between participants. There are several modified NIRS approaches capable of measuring these quantities, most of which have found limited use due to higher costs and lack of availability of necessary technology.

Additionally, there remains much work to be done in describing NIRS signals in the context of pulmonary gas exchange measurements beyond VO_2. In this area, a major hypothesis is that exercise related changes in arterial P_{CO2} will lead to changes in cerebral perfusion (36). Studies have suggested that there is a temporal correlation between threshold events that are observed during incremental exercise in both ventilation and tissue oxygenation as measured by NIRS (2, 28, 32). Such observations suggest a relationship between cardiorespiratory fitness and cerebral vascular function during exercise, but the methods used to investigate such correlations are to this day often based on visual inspection of NIRS data to identify thresholds (29). Given that the noise in breath-by-breath data obtained from children and performing exercise can significantly affect interpretation of data (31), it is likely that methods based on visual inspection are inadequate for reliable threshold modeling in pediatric participants. In our study, we have applied a computational tool for segmented regression to both breath-by-breath data and optical signals in order to address this concern.

The approach used in this study is known as time-resolved spectroscopy (TR-NIRS), and is beginning to find use in exercise physiology more frequently (1, 19). TR-NIRS can be used to quantify tissue concentrations of oxyhemoglobin ($[HbO_2]$), deoxyhemoglobin ([HbR]), and total hemoglobin ([THb]). From these, oxygen saturation is also calculated (stO_2, $100 \times [HbO_2]/[THb]$). We used TR-NIRS to measure tissue oxygenation in quadriceps (vastus lateralis, VL) and prefrontal cortex (PFC) in a group of healthy male children and

adolescents. Our objectives were: 1) To record absolute hemoglobin concentrations and oxygenation states and the magnitudes of changes at all stages of incremental exercise and 2) to study individual TR-NIRS and gas exchange curves using segmented regression to elucidate relationships between threshold events observed in tissue oxygenation and ventilation. This latter objective includes testing for a hypothesized relationship between ventilation and cerebral oxygenation, as well as exploratory analysis of potential correlations between muscle and cerebral oxygenation.

Methods

Exercise Studies

Eleven male children and adolescents (Table 1, mean age 15.33 ± 2.11 years, mean BMI = 21.09 ± 2.43) were recruited for the study. In each case, a parent provided written informed consent for participation, and each child provided assent. Studies were conducted in the early to mid-afternoon in the UC Irvine Pediatric Exercise Research Center under the supervision of an exercise physiologist. After vital signs were measured and evaluation for contraindications to exercise (eg injury, hyperthermia) was performed, each participant rested for 15 minutes. Participants sat on a stationary cycle and were fitted with surface electrodes for heart rate and rhythm recording; a mouthpiece for expired gas collection was placed and connected to a metabolic cart system (Vmax Encore 229, CareFusion) for breath-by-breath pulmonary gas exchange measurement by aspiration of small volumes from the expirate. Both gas analyzers and flow sensors were calibrated prior to each test. The testing protocol was then started as follows: 3-min baseline, with participants sitting still on the bike; 3-min unloaded warm-up; incremental exercise phase, during which resistance was increased continuously at a rate based on participant age, height, weight, and predicted VO_2 (45), and rounded to the nearest multiple of five (15 or 20 W/min). Each participant was instructed to maintain a cycling rate of 60-80 revolutions per minute, as indicated on the ergometer display. Peak performance was determined to be at the point of volitional exhaustion or the inability to maintain a cycling speed above 45 rpm. At this point, resistance was reduced to zero, and participants were asked to continue unloaded pedaling for three minutes after momentarily stopping. Finally, at 3 minutes post-exercise, participants were asked to stop pedaling, and TR-NIRS measurements continued for 3 additional minutes. Table 1 shows values of physiological parameters at peak exercise intensity for all participants.

TR-NIRS Measurements

The dual channel TRS-20 instrument (Hamamatsu Photonics, Japan) was calibrated using fixed-distance cylinders for measuring instrument function, after an initial warm-up period. During rest on the cycle, TR-NIRS probes were placed superior to the left PFC, as close as possible to the hairline, and lateral so as to avoid measuring over cerebral sinuses (30). The second channel probe was placed on the VL muscle on the anterolateral aspect of the thigh, midway between the anterior superior iliac spine and the patella. The source-detector separation used was three cm, and data was recorded every 3 seconds. The TRS-20 uses light of three wavelengths in each channel (759, 796, and 833 nm), and calculates absorption and scattering continuously at each one. Both probes were secured to the skin using double

sided adhesive, and an elastic headband was used to limit motion and ensure proper contact on the forehead probe. Using the TRS-20 software, data were processed by fitting to the diffusion approximation with mean photon path length (PL) to calculate scattering (reduced scattering coefficient, $\mu_{s'}$) and absorption (μ_a) at each measurement point and for each wavelength. These values were then used to calculate absolute concentrations of [HbO_2] and [HbR], and [THb]. Using these values, oxygen saturation is also calculated (stO_2, [HbO_2] / [THb]). When used in the muscle, TR-NIRS is incapable of separating oxygenated and deoxygenated forms of hemoglobin from myoglobin, respectively, and so total concentrations include a contribution from myoglobin. Values for path length and $\mu_{s'}$ at the 796 nm wavelength were also analyzed over the course of incremental exercise to determine if these parameters changed significantly

Data Analysis

Stage-by-stage oxygenation—First, TR-NIRS parameters at each stage were calculated by averaging 20 seconds of oxygenation data from TRS-20 control software at baseline (BL), unloaded pedaling (UP), and at several fractional stages of peak exercise time, and recovery, as follows: (20% peak (E20), 50% peak (E50), 80% peak (E80), peak time (PK), 2 minutes post (PT2), and 5 minutes post (PT5)) for each participant. $\mu_{s'}$ due to lower signal-to-noise ratio, was analyzed only at three time points: BL, E50, and PK. A linear mixed model was used to evaluate differences in TR-NIRS parameters among the 8 exercise/recovery stages (3 for $\mu_{s'}$) and repeated measurements were modeled with unrestricted covariance structure. *Post hoc* pairwise comparisons between all exercise stages were performed and p-values were adjusted using Bonferroni's method. The mean level, standard error (SE), and corresponding 95% confidence interval (CI) were all obtained from the linear mixed model. This analysis was performed using SAS 9.4 (Cary, NC) and the significance level was set at 0.05.

Threshold analysis—Threshold events in breath-by-breath gas exchange data and TR-NIRS data during only the incremental phase of exercise were identified using a segmented regression method. This was done using a tool called Shape Language Modeling (SLM, D'Errico, John. (2009) http://www.mathworks.com/matlabcentral/fileexchange/24443. Retrieved 2/19/2013). Shape language modeling is a computational package implemented in MATLAB that allows for iterative determination of optimal breakpoints between linear segments in longitudinal data, and which we have previously used to study data from other exercise paradigms (17). TR-NIRS thresholds were identified and characterized in PFC [HbO_2] (a change to negative slope late in exercise), PFC [HbR] (a change from steady-state to positive slope), and VL [THb] (change to steady-state or decline). For gas exchange data, VE and PET_{CO2} were used to identify the second ventilatory threshold (sometimes referred to as gas exchange threshold, or GET) in each test using the same piecewise method. This threshold is defined empirically as the point at which PET_{CO2} begins to decline, and when VE begins to increase at a faster rate late in incremental exercise.

Prior to segmented regression, each raw data set was also filtered using a moving window Hampel Filter to remove outliers, defined as points more than 2.5 standard deviations away from the mean of the window (Outlier Detection and Removal, Nielsen, Michael Lindholm.

(2012). http://www.mathworks.com/matlabcentral/fileexchange/34795-outlier-detection-and-removal-hampel. Retrieved 3/15/2013). Then, all data sets were smoothed using a local regression method with a span of 9 measurements. For each tracing, the SLM method uses as input a "knots" parameter which specifies the number of breakpoints between linear segments, and which was determined for each tracing by visual inspection. Then, the method iteratively fits the optimal linear segments to the data, such that the maximal R_2 value is achieved. The output of each fit includes the position in time of the breakpoints. These detected breakpoints in gas-exchange data and TR-NIRS measurements were expressed as a fraction of total exercise time achieved. The relationship of threshold time between gas-exchange measurements and TR-NIRS measurements were then evaluated using the Pearson's correlation.

RESULTS

Participant characteristics and peak performance parameters obtained from incremental tests are shown in table 1.

Tissue oxygenation dynamics: general

Figure 1 shows example tracings in both PFC and VL for all TR-NIRS variables. Figure 2 shows means and 95% CIs for all 11 participants at the 8 averaged stages: baseline, unloaded pedaling, 20%, 50%, 80% and 100% of total exercise time, and 2 and 5 min post (BL, UP, E20, E50, E80, PK, PT2, and PT5, respectively).

Tissue oxygenation dynamics: PFC

During exercise, PFC [HbO_2] increased significantly over BL, with the greatest increase observed at E80, +6.3±1.0 μM, ($p < 0.002$, Fig 2A). [HbR] in the PFC also increased over BL, reaching significance at PK (+5.9±1.4 μM, $p < 0.05$) and at PT2 (+8.0±1.2 μM, $p<0.002$, Fig 2B). [THb] in the PFC began to increase after E50, and remained elevated through recovery (E50, +5.3 ± 0.7 μM, $p < 0.001$; PT2, +12.3 ± 2.2 μM, $p < 0.01$). Oxygen saturation was unchanged until E80, thereby dropping by 3.0 ± 0.5 μM at PK ($p < 0.01$), and remaining 3.79 ± 0.62 μM lower than BL through PT2 ($p < 0.005$).

Tissue oxygenation dynamics: VL

VL [HbO_2] (Fig 2E) decreased slightly and non-significantly during exercise, and thereafter increased rapidly, from PK to PT2, by 13.0 ± 2.0 μM ($p < 0.005$). VL [HbR] (Fig, 2F) increased significantly in the middle stages of exercise (+8.0 ± 1.3 μM, $p < 0.005$ E80 vs UP), reached a plateau between E80 and PK, and decreased to 7.2 ± 1.6 μM below BL ($p < 0.05$ PT5 vs BL). VL [THb], Fig. 2G, increased significantly from UP to E80 (+6.99 ± 0.84 μM, $p < 0.001$), and did not significantly change subsequently. VL stO_2 decreased progressively through exercise, reaching the largest drop below UP at PK (-- 6.8 ± 1.45 μM, $p<0.05$), and then increase through recovery (+13.5 ± 1.7 μM, $p < 0.002$, PT5 vs PK).

Changes in optical path length (PL) and scattering

Path length at 796 nm declined significantly during exercise in both tissues. In the VL, path length at E50 and all subsequent stages was lower than the baseline value (from 14.90 cm at

BL to 14.56 at E80, $p < .001$). In the PFC, this occurred at E80 and all subsequent points (from 15.39 cm at BL to 15.13 cm at 0.8 PK, $p < .05$). The scattering coefficient, μ_s', (assessed at only BL, E50, and PK) increased in the PFC in the latter half of exercise (from 10.46 cm^{-1} to 10.65 cm^{-1}, E50 vs PK, $p < .05$), and decreased in the VL in the first half of exercise (from 8.54 cm^{-1} to 8.36 cm^{-1}, UP v. E50, $p < .005$).

Threshold analysis

On average, the VL [THb] threshold (transition from positive slope to steady state or negative slope) occurred at 73 ± 13 % of total exercise time. The PFC [HbR] threshold (transition from small positive slope or flat line to larger positive slope) occurred at 70 ± 7 % of total exercise time, and the PFC [HbO_2] threshold (transition from positive slope to zero or negative slope late in exercise) occurred at 80 ± 7 % of total exercise time.

Correlations between Hb thresholds and ventilatory parameters

The above Hb thresholds were tested for correlation with the second ventilatory threshold, identified in tracings of PET_{CO2} and VE. Strong correlations were identified between the PFC [HbO_2] threshold and the negative inflection in the slope of PET_{CO2} ($r = 0.84$), and the increased positive slope of VE ($r = .87$) (Fig. 3B and 3C). There were 2 participants in whom the threshold could not be resolved from the piecewise regression model. When examining the data visually, one revealed no such transitions in either PET_{CO2} or [HbO_2] in the late stages of exercise and in the other, there was a decline in [HbO_2] at 0.91 of total exercise time, but a change to steeper positive slope in PET_{CO2} at a similar time (0.84 of total time).

Exploratory analysis also found a moderate correlation between thresholds in VL [THb] and PFC [HbR] ($r = .73$), indicating that the transition to steady state or negative slope in VL [THb] appears to occur at a similar time with the transition to more steeply increasing PFC [HbR]. Figure 4A & B depicts this in two representative participants. Further analysis of the VL [THb] threshold indicates that the magnitude of the decline in [THb] from the threshold to PK is positively correlated with individual peak VO_2 (Fig 4C).

Discussion

In this study, we demonstrated that significant changes in absolute hemoglobin concentrations, oxygenation, and optical PL and μ_s' occur simultaneously in the exercising muscle and brain of children during incremental cycling and post-exercise recovery. We also identified physiological thresholds that can be detected in both VL and PFC TR-NIRS data, the temporal relation of these thresholds to one another, and to systemic physiological responses, such as VE and PET_{CO2}.

Muscle Oxygenation

In our study a significant and progressive decrease in stO_2 occurred during the middle stages of incremental exercise. This was accompanied by an increase in [THb] from UP to E80. This change in [THb] was driven by a large increase in [HbR], and in absolute terms, a smaller decrease in [HbO_2]. These findings are consistent with those recently reported in

ramp exercise in adults, demonstrating general agreement with existing continuous wave NIRS methodologies (13, 14).

With regard to threshold analysis, we also observed that during each incremental test VL [THb], an index of total blood volume in muscle tissue (42), after a steady initial increase, reached a point beyond which it remained constant or declined from a peak value. Further analysis showed that participants either demonstrated a noticeable drop in VL [THb] from the threshold value to the end of ramp exercise (n = 5, ranging from −6.6% to −9.0%), or little to no change (n = 6, ranging from −1.1% to +1.1%). The participants who demonstrated larger drops in VL [THb] tended to also have higher levels of peak aerobic fitness, achieving peak V_{O2} values of > 40 ml/min/kg (Fig. 4C). In incremental cycling, leg vascular conductance and blood flow are known to reach maxima before V_{O2} peak (24), possibly due to the increasing sympathetic vasoconstriction in the later stages of exercise, which dampens the O_2 demand-driven vasodilation that occurs during the earlier stages of exercise (24). We can speculate that the threshold in muscle [THb] we observed corresponds to a maximum in vascular conductance reached in the incremental test, or perhaps a point after which hematocrit reaches a plateau (10). Other invasive methods must be used to confirm this in future studies. If the VL [THb] threshold represents a maximum in the delivery of O_2 to the muscle (5, 32), then the correlation between the subsequent drop in [THb] with peak VO_2 indicates that higher fitness is associated with greater tolerance for exercise beyond this limit. In this study, only one location on the VL was measured, and therefore we cannot address any potential effects of dynamic spatial heterogeneity in the exercising muscles of the leg (7, 19), nor the inhomogeneity introduced by variations in subcutaneous tissue thickness (6) or skin blood flow (21). Nonetheless, based on these results, the assessment of the [THb] threshold in exercising muscle during incremental tests may be a way to evaluate muscle vascular adaptation to exercise.

Furthermore, an exploratory analysis demonstrated a significant correlation between the timing of the VL [THb] threshold and the time at which PFC [HbR] begins to increase more steeply (r = .73). The observation that this muscle [THb] threshold correlates with the onset of faster O_2 extraction in the PFC is of interest, but is not explained easily. Other investigators have suggested the possibility that sympathetic nervous activity can affect cerebral metabolism (37), and we might therefore speculate that this explains the concurrence of the [THb] threshold and accelerated PFC [HbR] increase.

PFC Oxygenation

The typical pattern of NIRS measurements in the PFC during ramp exercise is an increase in both [HbR] and [HbO_2] with increasing intensity, with a possible decline in [HbO_2] and stO_2 at the highest intensities depending on age and training status (33, 34). It is hypothesized by some that this decline in stO_2 may be a limiting factor in exercise performance (33, 34, 39), however the published evidence is not conclusive (39). Other studies have shown that intense exercise is associated with an increase in regional cerebral blood flow (CBF) using techniques such as Trans-Cranial Doppler Ultrasound and clearance of ^{133}Xe (36). More recently, Vogiatzis et al showed that in athletes, incremental exercise is associated with an increase in frontal cortex blood flow, with a relative reduction at the

highest intensities when exercise was performed under hypoxic conditions (44). Similar findings were recently reported in a group of adult participants, in which low-intensity exercise increased cerebral vascular conductance (16) (at least in young individuals), while higher work intensities induced a decline in cerebral vascular conductance in both old and young adults (16), a decline attributed to the simultaneous decrease in arterial CO_2 content, caused by hyperventilation late in exercise (16). Taken together, these and other studies point to an increase in cerebral vascular conductance and blood volume at lower intensities, with a likely decrease at the highest intensities.

In our study, the level of [THb], which has been tied to the level of cerebral blood volume (33), also increased and seemed to plateau above E80, remaining elevated for at least the first 5 min after exercise cessation. On average, we also observed an absolute decline in stO_2 beginning at E80. Others have suggested that PFC stO_2 declines in late exercise in response to hyperventilation and decreased PET_{CO2} (2). Because stO_2 is sensitive to changes in both [HbO_2] and [HbR], we chose to analyze [HbO_2] specifically because it tends to more closely follow perfusion (20). The high degree of temporal correlation between the point at which PET_{CO2} declines and the point at which PFC [HbO_2] declines ($r = 0.84$) would lend evidence to a relationship between the drop in PET_{CO2} and PFC perfusion late in incremental exercise.

PFC [HbR] in most participants seemed to behave differently from [HbO_2], following as determined by segmented linear regression, with slow and fast phases of increase. The fast phase began at an average of 70% of PK ($\sigma = 8$ %), indicating an increased rate of cerebral O_2 metabolism (16). With regard to brain metabolism, Secher et al (36, 37) have extensively reviewed concepts of cerebral metabolism in exercise. There is evidence of both regional increases in anaerobic metabolism, as well as increased glycolysis and oxidation of lactate late in exercise (37). These changes, although still incompletely understood, appear related to increased lactate availability, and perhaps increased sympathetic activity. We can speculate that the changes observed in PFC [HbR] in our study are driven by the well-known delayed accumulation of blood lactate. Interestingly, PFC [THb] and [HbR] also remained significantly elevated for several minutes post-exercise (12.3 and 8.0 μM higher, $p = .0062$ and .0014, respectively, at PT2). PFC stO_2 was also significantly lower (3.8% less than BL, $p = .0034$) in the first minutes post-exercise, perhaps reflecting excess post-exercise oxygen consumption in PFC (9). It should also be noted that PFC [HbO_2] decline occurs in the context of a continuously increasing [HbR], perhaps indicating an early discrepancy between continuously increasing metabolism and a limitation in perfusion. While not conclusive, this leaves open the possibility that the decline in [HbO_2] is predictive of test cessation.

Changes in optical path length and scattering

We found that exercise is associated with changes in PL and $\mu_{s'}$ in both tissues. One potential explanation for a change in PFC PL and scattering is a change in cerebral fluid distribution with exercise. It has been shown that in mice, brain edema is associated with a measurable increase in scattering properties (43). Other hypotheses for changes in scattering with exercise are speculative (including changes in hematocrit and blood density), and warrant further investigation, combined with other measurements, such as intracranial pressure. In

the case of exercising muscle, the overall picture is different. Ferrari et al reported that using a frequency-domain NIRS device, the assumption of constant scattering results in overestimation in the change in both [HbO_2] and [HbR] in the exercising muscle (13). In contrast to the values reported here, the same study also reported that exercise was associated with an increase in muscle μ_s'. Given the significant changes in PL and μ_s', it is possible that continuous wave NIRS methods would interfere with detection of NIRS threshold events during incremental exercise, such as has been suggested in another published report involving a steady-state exercise challenge (35).

Correlations between gas exchange and TR-NIRS measurements

As figure 3 demonstrates, there are TR-NIRS variables that show correlation with gas exchange parameters over the whole duration of incremental exercise. However, a more careful analysis would take into account the known threshold behavior observed in incremental exercise. To that end, we have used a computational approach to determine whether there are correlations between threshold events in physiological data collected by different instruments and at different sites. This method provided iterative determination of the optimal points of slope changes between linear segments. We also applied the same technique to the study of pulmonary gas exchange data to make correlations between established ventilatory transitions and TR-NIRS measurements. While the use of this particular software tool in physiology is relatively novel, the concept of threshold modeling is not. Incremental exercise is frequently modeled by division into three phases by identifying two ventilatory thresholds, or increases in the rate of ventilation (3). A similar approach was used to identify transition times in both heart rate and oxygenation data in incremental exercise (22). They found, using a two-linear phase approach, that quadriceps oxygenation changes were correlated in time to the onset of slope changes in HR. This approach was successful, despite the observation that in later stages of exercise, HR does not follow first degree kinetics; indeed, others have described the HR transition as a loss of the linear relationship between HR and work rate (4). There have been other methods recently described to conduct similar breakpoint analyses in exercise physiology recently (32). While the piecewise linear approach does not achieve full mathematical description of physiological kinetics (38), it is useful in the identification of transitions between phases, which are frequently described in a variety of exercise paradigms (28, 29).

Limitations

There are several factors that must be considered in drawing conclusions from these results. First, we have speculated that the VL [THb] threshold represents a maximum in exercising muscle vascular conductance. However, it has been shown that muscle [THb] changes are not driven only by changes in perfusion or vascular conductance, but also by the level of myoglobin in the muscle, as well as changes in hematocrit (10) that are known to occur in intense exercise. Additionally, in this study there was no correction for differences in adipose tissue thickness between participants, as has been demonstrated in other studies (27). This likely explains the large range of VL [THb] values at BL. Both of the above limitations are common to all muscle NIRS studies. Additionally, as described above, the SLM method was not successful in identifying PET_{CO2}, VE, and PFC [HbO_2] thresholds in all participants, which may have been due to noise in the data or perhaps a lack of

occurrence in those particular tests. And finally, while the participant population was homogenous in gender (male) and relatively close in age, the sample size was still somewhat small.

In summary, despite these limitations, our findings show that significant changes occur in VL and PFC oxygenation in adolescents performing and recovering from intense exercise, and that the magnitude of these changes can be quantified using TR-NIRS. Threshold analysis of TR-NIRS data in exercising adolescents reveals potential relationships between ventilation and cerebral perfusion, as well as muscle vascular conductance and peak performance.

Acknowledgements

We gratefully acknowledge Scott Graf for operating the metabolic cart from which gas exchange data was collected for these studies. We also acknowledge the research nursing staff for assistance with research participants. We also acknowledge Hamamatsu Photonics for assistance with the TRS-20 instrument used in these studies. Finally, the UC Irvine Pediatric Exercise Research Center is acknowledged for providing facilities for the conducting of these exercise studies.

Funding:

This research was funded by the National Institutes of Health through an NIH TL-1 fellowship, 8UL1TR000153 (GG), and research grant NIH P01D048721 (PG). Support was also provided by institutional grants: P41EB015890 (BJT), and UL1TR000153 (DC); and the Arnold and Mabel Beckman Foundation.

Abbreviations

PFC	Prefrontal cortex
VL	Vastus Lateralis
BL	Baseline
UP	Unloaded pedaling
E0	Onset of resistance
E20	20% of total ramp exercise time
E40	40% of total ramp time
E60	60% of total ramp time
E80	80% of total ramp tme
PK	Peak exertion (total exercise time)
NIRS	Near-infrared spectroscopy
[HbR]	Deoxyhemoglobin
[HbO_2]	Oxyhemoglobin
[THb]	Total hemoglobin
stO_2	Oxygen saturation
TR-NIRS	Time-resolved near-infrared spectroscopy

References

1. Adami A, Koga S, Kondo N, Cannon DT, Kowalchuk JM, Amano T, et al. Changes in whole tissue heme concentration dissociates muscle deoxygenation from muscle oxygen extraction during passive head-up tilt. J Appl Physiol. 2015; 118(9):1091–9. [PubMed: 25678700]
2. Bhambhani Y, Malik R, Mookerjee S. Cerebral oxygenation declines at exercise intensities above the respiratory compensation threshold. Respir Physiol & Neurobiol. 2007; 156(2):196–202. [PubMed: 17045853]
3. Blain G, Meste O, Bouchard T, Bermon S. Assessment of ventilatory thresholds during graded and maximal exercise test using time varying analysis of respiratory sinus arrhythmia. Br J Sports Med. 2005; 39(7):448–52. discussion -52. [PubMed: 15976169]
4. Bodner ME, Rhodes EC. A review of the concept of the heart rate deflection point. Sports Med. 2000; 30(1):31–46. [PubMed: 10907756]
5. Boone J, Barstow TJ, Celie B, Prieur F, Bourgois J. The impact of pedal rate on muscle oxygenation, muscle activation and whole-body VO(2) during ramp exercise in healthy subjects. Eur J Appl Physiol. 2015; 115(1):57–70. [PubMed: 25204279]
6. Bowen TS, Rossiter HB, Benson AP, Amano T, Kondo N, Kowalchuk JM, et al. Slowed oxygen uptake kinetics in hypoxia correlate with the transient peak and reduced spatial distribution of absolute skeletal muscle deoxygenation. Exp Physiol. 2013; 98(11):1585–96. [PubMed: 23851917]
7. Chin LM, Kowalchuk JM, Barstow TJ, Kondo N, Amano T, Shiojiri T, et al. The relationship between muscle deoxygenation and activation in different muscles of the quadriceps during cycle ramp exercise. J Appl Physiol. 2011; 111(5):1259–65. [PubMed: 21799133]
8. Clark MG. Impaired microvascular perfusion: a consequence of vascular dysfunction and a potential cause of insulin resistance in muscle. Am J Physiol Endocrinol Metab. 2008; 295(4):E732–50. [PubMed: 18612041]
9. Danduran MJ, Dixon JE, Rao RP. Near Infrared Spectroscopy Describes Physiologic Payback Associated With Excess Postexercise Oxygen Consumption in Healthy Controls and Children With Complex Congenital Heart Disease. Pediatr Cardiol. 2011
10. Davis ML, Barstow TJ. Estimated contribution of hemoglobin and myoglobin to near infrared spectroscopy. Respir Physiol & Neurobiol. 2013; 186(2):180–7. [PubMed: 23357615]
11. Dogra S, Spencer MD, Murias JM, Paterson DH. Oxygen uptake kinetics in endurancetrained and untrained postmenopausal women. Appl Physiol Nutr Metab. 2013; 38(2):154–60. [PubMed: 23438226]
12. Ekkekakis P. Illuminating the black box: investigating prefrontal cortical hemodynamics during exercise with near-infrared spectroscopy. J Sport Exerc Psychol. 2009; 31(4):505–53. [PubMed: 19842545]
13. Ferreira LF, Hueber DM, Barstow TJ. Effects of assuming constant optical scattering on measurements of muscle oxygenation by near-infrared spectroscopy during exercise. J Appl Physiol. 2007; 102(1):358–67. [PubMed: 17023569]
14. Ferreira LF, Koga S, Barstow TJ. Dynamics of noninvasively estimated microvascular O2 extraction during ramp exercise. J Appl Physiol. 2007; 103(6):1999–2004. [PubMed: 17823295]
15. Ferreira LF, Townsend DK, Lutjemeier BJ, Barstow TJ. Muscle capillary blood flow kinetics estimated from pulmonary O2 uptake and near-infrared spectroscopy. J Appl Physiol. 2005; 98(5): 1820–8. [PubMed: 15640391]
16. Fisher JP, Hartwich D, Seifert T, Olesen ND, McNulty CL, Nielsen HB, et al. Cerebral perfusion, oxygenation and metabolism during exercise in young and elderly individuals. J Physiol. 2013; 591:1859–70. Pt 7. [PubMed: 23230234]
17. Ganesan G, Cotter JA, Reuland W, Cerussi AE, Tromberg BJ, Galassetti P. Effect of blood flow restriction on tissue oxygenation during knee extension. Med Sci Sports Exerc. 2015; 47(1):185–93. [PubMed: 24870580]
18. Habazettl H, Athanasopoulos D, Kuebler WM, Wagner H, Roussos C, Wagner PD, et al. Near-infrared spectroscopy and indocyanine green derived blood flow index for noninvasive measurement of muscle perfusion during exercise. J Appl Physiol. 2010; 108(4):962–7. [PubMed: 20110542]

19. Koga S, Poole DC, Fukuoka Y, Ferreira LF, Kondo N, Ohmae E, et al. Methodological validation of the dynamic heterogeneity of muscle deoxygenation within the quadriceps during cycle exercise. Am J Physiol Regul Integr Comp Physiol. 2011; 301(2):R534–41. [PubMed: 21632845]
20. Lee J, Kim JG, Mahon S, Tromberg BJ, Ryan KL, Convertino VA, et al. Tissue hemoglobin monitoring of progressive central hypovolemia in humans using broadband diffuse optical spectroscopy. J Biomed Opt. 2008; 13(6):064027. [PubMed: 19123673]
21. Messere A, Roatta S. Influence of cutaneous and muscular circulation on spatially resolved versus standard Beer-Lambert near-infrared spectroscopy. Physiol Rep. 2013; 1(7):e00179. [PubMed: 24744858]
22. Mizuno M, Tokizawa K, Iwakawa T, Muraoka I. Inflection points of cardiovascular responses and oxygenation are correlated in the distal but not the proximal portions of muscle during incremental exercise. J Appl Physiol. 2004; 97(3):867–73. [PubMed: 15107412]
23. Moalla W, Dupont G, Temfemo A, Maingourd Y, Weston M, Ahmaidi S. Assessment of exercise capacity and respiratory muscle oxygenation in healthy children and children with congenital heart diseases. Appl Physiol Nutr Metab. 2008; 33(3):434–40. [PubMed: 18461095]
24. Mortensen SP, Damsgaard R, Dawson EA, Secher NH, Gonzalez-Alonso J. Restrictions in systemic and locomotor skeletal muscle perfusion, oxygen supply and VO2 during high-intensity whole-body exercise in humans. J Physiol. 2008; 586(10):2621–35. [PubMed: 18372307]
25. Murias JM, Spencer MD, Delorey DS, Gurd BJ, Kowalchuk JM, Paterson DH. Speeding of VO2 kinetics during moderate-intensity exercise subsequent to heavy-intensity exercise is associated with improved local O2 distribution. J Appl Physiol. 2011
26. Murias JM, Spencer MD, Kowalchuk JM, Paterson DH. Muscle deoxygenation to VO(2) relationship differs in young subjects with varying tauVO(2). Eur J Appl Physiol. 2011
27. Ohmae E, Nishio S, Oda M, Suzuki H, Suzuki T, Ohashi K, et al. Sensitivity correction for the influence of the fat layer on muscle oxygenation and estimation of fat thickness by time-resolved spectroscopy. J Biomed Opt. 2014; 19(6):067005. [PubMed: 24911021]
28. Oussaidene K, Prieur F, Bougault V, Borel B, Matran R, Mucci P. Cerebral oxygenation during hyperoxia-induced increase in exercise tolerance for untrained men. Eur J Appl Physiol. 2013; 113(8):2047–56. [PubMed: 23579360]
29. Oussaidene K, Prieur F, Tagougui S, Abaidia A, Matran R, Mucci P. Aerobic fitness influences cerebral oxygenation response to maximal exercise in healthy subjects. Respir Physiol & Neurobiol. 2015; 205:53–60. [PubMed: 25461626]
30. Perrey S. Non-invasive NIR spectroscopy of human brain function during exercise. Methods (San Diego, Calif). 2008; 45(4):289–99.
31. Potter CR, Childs DJ, Houghton W, Armstrong N. Breath-to-breath “noise” in the ventilatory and gas exchange responses of children to exercise. Eur J Appl Physiol Occup Physiol. 1999; 80(2): 118–24. [PubMed: 10408322]
32. Racinais S, Buchheit M, Girard O. Breakpoints in ventilation, cerebral and muscle oxygenation, and muscle activity during an incremental cycling exercise. Front Physiol. 2014; 5:142. [PubMed: 24782786]
33. Rooks CR, Thom NJ, McCully KK, Dishman RK. Effects of incremental exercise on cerebral oxygenation measured by near-infrared spectroscopy: a systematic review. Prog Neurobiol. 2010; 92(2):134–50. [PubMed: 20542078]
34. Rupp T, Perrey S. Prefrontal cortex oxygenation and neuromuscular responses to exhaustive exercise. Eur J Appl Physiol. 2008; 102(2):153–63. [PubMed: 17882449]
35. Saitoh T, Ooue A, Kondo N, Niizeki K, Koga S. Active muscle oxygenation dynamics measured during high-intensity exercise by using two near-infrared spectroscopy methods. Adv Exp Med Biol. 2010; 662:225–30. [PubMed: 20204796]
36. Secher NH, Seifert T, Van Lieshout JJ. Cerebral blood flow and metabolism during exercise: implications for fatigue. J Appl Physiol. 2008; 104(1):306–14. [PubMed: 17962575]
37. Seifert T, Secher NH. Sympathetic influence on cerebral blood flow and metabolism during exercise in humans. Prog Neurobiol. 2011; 95(3):406–26. [PubMed: 21963551]

38. Spencer MD, Murias JM, Paterson DH. Characterizing the profile of muscle deoxygenation during ramp incremental exercise in young men. Eur J Appl Physiol. 2012; 112(9):3349–60. [PubMed: 22270488]

39. Subudhi AW, Olin JT, Dimmen AC, Polaner DM, Kayser B, Roach RC. Does cerebral oxygen delivery limit incremental exercise performance? J Appl Physiol. 2011; 111(6):1727–34. [PubMed: 21921244]

40. Taelman J, Vanderhaegen J, Robijns M, Naulaers G, Spaepen A, Van Huffel S. Estimation of muscle fatigue using surface electromyography and near-infrared spectroscopy. Adv Exp Med Biol. 2011; 701:353–9. [PubMed: 21445809]

41. Tempest GD, Eston RG, Parfitt G. Prefrontal cortex haemodynamics and affective responses during exercise: a multi-channel near infrared spectroscopy study. PLoS One. 2014; 9(5):e95924. [PubMed: 24788166]

42. Tew GA, Ruddock AD, Saxton JM. Skin blood flow differentially affects near-infrared spectroscopy-derived measures of muscle oxygen saturation and blood volume at rest and during dynamic leg exercise. Eur J Appl Physiol. 2010; 110(5):1083–9. [PubMed: 20700602]

43. Thiagarajah JR, Papadopoulos MC, Verkman AS. Noninvasive early detection of brain edema in mice by near-infrared light scattering. J Neurosci Res. 2005; 80(2):293–9. [PubMed: 15765520]

44. Vogiatzis I, Louvaris Z, Habazettl H, Athanasopoulos D, Andrianopoulos V, Cherouveim E, et al. Frontal cerebral cortex blood flow, oxygen delivery and oxygenation during normoxic and hypoxic exercise in athletes. J Physiol. 2011; 589:4027–39. Pt 16. [PubMed: 21727220]

45. Wasserman K, Hansen JE, Sue DY, Whipp BJ, Froelicher VF. Principles of exercise testing and interpretation. J Cardiopulm Rehabil Prev. 1987; 7(4):189.

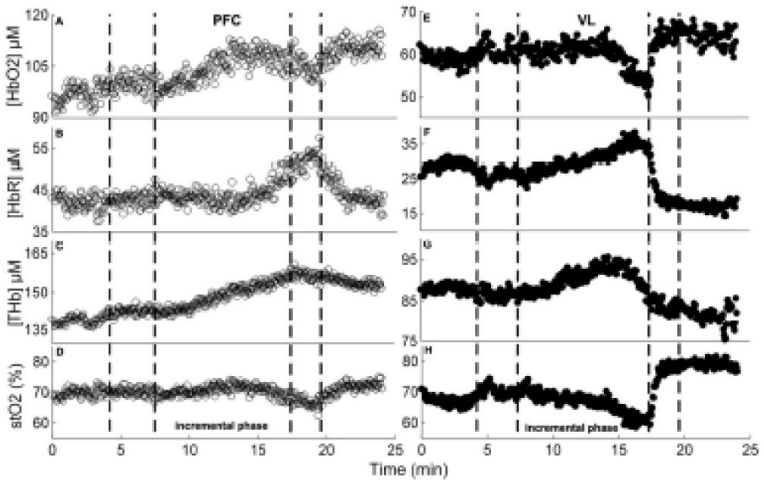

Figure 1.

(A) - (D) show representative tracings for absolute [HbO_2], [HbR], [THb], and stO2 respectively in one participant. Vertical dashed lines delineate stages of exercise (Baseline, unloaded pedaling, incremental phase, recovery pedaling, and full rest). Within each plot, hollow circles denote traces from PFC, while filled circles are from VL.

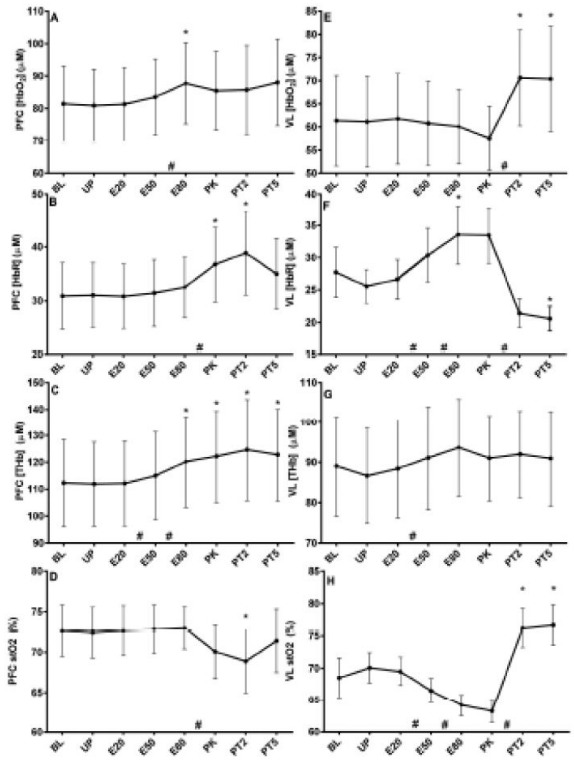

Figure 2.

Sample means ± 95% CIs for [HbO_2], [HbR], [THb], and stO_2 in PFC (A – D) and VL (E – H). BL = baseline, UP = unloaded pedaling, E20 = 20% total time, E50 = 50% total time, E80 = 80% total time, PK = total time of exercise (time to peak work rate), PT2 = 2 minutes post, and PT5 = 5 minutes post. * = $p < .05$ vs. BL. # = $p < .05$ between consecutive data points.

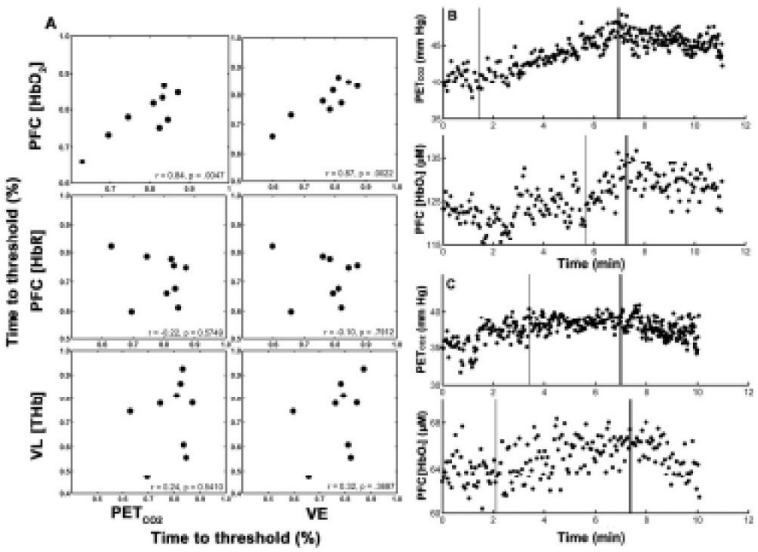

Figure 3.

A shows Pearson Product correlation between relative threshold times in PFC [HbO_2] (top), PFC [HbR] (middle), and VL [THb] (bottom), and the second ventilatory threshold as detected in $PETCO_2$ (left column) and VE (right column). Fractional timings are normalized to total exercise time for each individual participant. B and C are representative piecewise fits for PET_{CO2} (top) and PFC [HbO_2] (bottom) for two participants. Thick vertical lines represent the detected breakpoints of interest, while thinner lines represent other breakpoints.

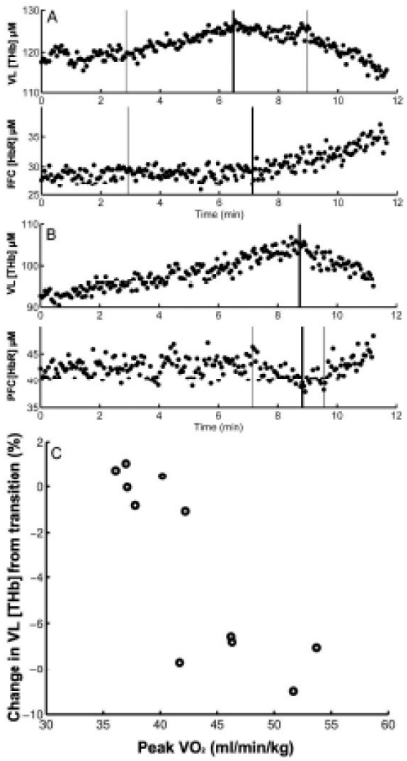

Figure 4.

A - B show representative piecewise fits of VL [THb] (top) and PFC [HbR] (bottom) in 2 participants. The thick vertical lines represent he detected breakpoints of interest, while the thinner lines represent other breakpoints. C shows scatter plot of peak VO_2 (ml/min/kg) achieved by individual participants on the x-axis, and the percentage drop of VL [THb] from peak for each corresponding participant on the y-axis.

Table 1

Participant characteristics and physiological parameters at maximal exercise time.

Subject	Age	Height (cm)	Weight (kg)	BMI Z-score	Peak VO2 (ml/min/kg)	Peak Work (Watts)	Total ramp time (min)	Peak HR
1	15.99	178	61.8	−0.41	53.7	237	12.26	193
2	17.54	162	58	0.18	46.2	197	10.18	181
3	16.42	178	61.5	−.55	42.2	190	13.10	196
4	17.13	177	74.7	0.76	37.1	212	11.07	193
5	13.32	172	65.1	0.61	46.3	206	11.22	182
6	10.44	146	49.7	1.29	40.2	131	10.07	183
7	17.27	170	63.9	1.56	36.1	170	11.79	194
8	14.5	159	62	.9	37	158	11.02	198
9	16.25	171	58.7	−.03	51.7	223	11.64	179
10	14.13	166	48.9	−.67	37.8	128	9.23	186
11	15.62	170	50.1	−1.61	41.7	144	9.97	194
Average	15.33	168.09	59.49		42.73	181.45	11.05	189.00
Std. Dev.	2.11	9.59	7.73		6.05	37.61	1.13	6.86